

A Comparative Analysis of Convolutional Neural Network Architectures for Breast Cancer Classification from Mammograms

Yigitcan Cakmak *,¹ and Javanshir Zeynalov ,²

*Department of Computer Engineering, Faculty of Engineering, Igdir University, 76000, Igdir, Türkiye, ^aDepartment of Electronics and Information Technologies, Faculty of Architecture and Engineering, Nakhchivan State University, AZ 7012, Nakhchivan, Azerbaijan.

ABSTRACT Breast cancer represents a significant global health challenge, ranking as one of the most prevalent malignancies among women. Early and accurate diagnosis through medical imaging is paramount for improving patient outcomes, with mammography serving as the gold standard for screening. However, the interpretation of mammograms can be challenging and subject to inter-observer variability. This study aims to comparatively evaluate the performance and computational efficiency of four prominent Convolutional Neural Network (CNN) architectures for the automated classification of breast cancer from mammogram images. Utilizing a publicly available dataset comprising 3,383 mammogram images classified as either Benign or Malignant, we trained and evaluated four distinct models: InceptionV3, DenseNet169, InceptionV4, and ResNet50. The results demonstrate that the DenseNet169 architecture achieved superior performance across all evaluated metrics, attaining the highest accuracy (73.33%), precision (70.45%), recall (67.83%), and F1-score (68.60%). Notably, DenseNet169 also exhibited the highest computational efficiency, featuring the lowest parameter count (12.49M) among the tested models. These findings suggest that DenseNet169 offers an optimal balance between diagnostic accuracy and model efficiency, positioning it as a highly promising candidate for integration into clinical decision support systems to aid radiologists in the early detection of breast cancer.

INTRODUCTION

Cancer represents one of the most complex and devastating diseases confronting modern medicine (García Megías *et al.* 2025). It is fundamentally a pathological condition characterized by the uncontrolled division and proliferation of the body's cells (Siqueira *et al.* 2024; Rezaei *et al.* 2025). Normally, healthy cells grow, divide, and die according to the body's needs. However, cancerous cells arise from genetic mutations that disrupt this regulated cycle, proliferating incessantly to form masses known as "tumors" (Sirvi *et al.* 2025; Yousefnia 2024). These tumors not only damage the tissue in which they are located but can also spread to other parts of the body via the blood or lymphatic system, a process known as "metastasis," thereby impairing the function of vital organs (Zuo *et al.* 2024; Li *et al.* 2025). According to World Health Organization (WHO) data, cancer is a leading cause of death globally, responsible for millions of fatalities each year (Mohanti *et al.* 2025; Lin and Park 2024). In the fight against this global health problem, understanding the biology of the disease is as crucial as achieving an early and accurate diagnosis in order to increase survival rates

and enhance treatment success (Mundel *et al.* 2023; Aggarwal and Bagri 2025).

Within this broad spectrum of cancer, breast cancer is distinguished as the most prevalent type, particularly among women (Kim *et al.* 2025; Xiong *et al.* 2025). Millions of women worldwide are diagnosed with breast cancer annually, and it is the leading cause of cancer-related mortality in this demographic. Breast cancer, which can develop due to a multitude of risk factors including genetic predisposition, hormonal factors, lifestyle, and environmental influences, is a disease that is highly responsive to treatment when detected at an early stage (Obeagu and Obeagu 2024). Early diagnosis ensures the tumor is identified when it is still small and has not spread to surrounding tissues (Kiani *et al.* 2025; Alshawwa *et al.* 2024; Begum *et al.* 2024). This enables the use of less invasive treatment methods and elevates five-year survival rates to over 90% (Katsika *et al.* 2024; Trentham-Dietz *et al.* 2024). Therefore, raising public awareness and expanding regular screening programs are regarded as the most effective strategies for reducing the mortality of the disease.

Among the various imaging techniques used for the early detection of breast cancer, mammography is the most common and effective method, widely recognized as the "gold standard" (Chandra *et al.* 2025). Mammography is a radiological technique that provides detailed imaging of the breast using low-dose X-rays (Dhamija *et al.* 2025). This method allows for the detection of

Manuscript received: 21 May 2025,

Revised: 19 June 2025,

Accepted: 12 July 2025.

¹ygtnckmak@gmail.com (Corresponding author)

²cavansirzeynalov@ndu.edu.az

KEYWORDS

Breast cancer
Deep learning
Mammography
Image classification
Computer-aided diagnosis (CAD)

masses too small to be palpated, architectural distortions, and especially microcalcification clusters (small calcium deposits), which can be an early sign of cancer (Al-Balas *et al.* 2024). However, the interpretation of mammography is a complex and subjective process that relies heavily on the radiologist's experience and diligence (Nicosia *et al.* 2024). Factors such as high workload, fatigue, or overlooking subtle details in the image can lead to false-negative (missing a cancer) or false-positive (suspecting cancer where there is none) results (Mousa *et al.* 2024; Bahrami *et al.* 2025). This situation can lead to unnecessary biopsies, anxiety for patients, or delays in treatment. These challenges have necessitated the development of a more objective, rapid, and reliable decision support system for the analysis of mammographic images.

In recent years, advancements in artificial intelligence (AI), particularly in the field of deep learning, have instigated a revolution in medicine, especially in medical image analysis (Pacal and Attallah 2025; Pacal 2025). Convolutional Neural Networks (CNNs), owing to their superior capability to learn hierarchical features from visual data, have demonstrated performance comparable to, and in some cases, superior to that of human experts in analyzing radiological images (Pacal *et al.* 2025; İnce *et al.* 2025; Bayram *et al.* 2025). CNN-based models can automatically learn the subtle and complex discriminative features of normal tissue patterns versus benign and malignant lesions from mammograms. Within the scope of this study, the potential of this technology has been leveraged for the detection of breast cancer from mammography images (Lubbad *et al.* 2024b; Kurtulus *et al.* 2024). To this end, four different deep learning (DL) architectures with proven success in the literature ResNet50, DenseNet169, InceptionV3, and InceptionV4 were utilized to classify mammogram images as benign (0) or malignant (1) (Cakmak *et al.* 2024; Ozdemir *et al.* 2025). The objective is to compare the performance of these models to identify the most effective AI approach that can serve as a robust second-opinion and decision support tool for radiologists (Cakmak and Pacal 2025; Zeynalov *et al.* 2025; Lubbad *et al.* 2024a).

The field of medicine is undergoing a transformative evolution with the integration of AI, particularly its subfields of DL and machine learning (ML) (Obuchowicz *et al.* 2024; Koçak *et al.* 2025). These technologies offer significant advancements across a wide range of applications, from the early diagnosis of diseases and the development of personalized treatment protocols to drug discovery and the analysis of complex biological data (Li *et al.* 2024; Islam *et al.* 2024). Medical imaging, in particular, holds immense potential due to the ability of AI algorithms to process vast amounts of data and detect patterns imperceptible to the human eye (Chambi *et al.* 2025; Meng *et al.* 2024). In this context, Sarvi *et al.* compared Mamba-based models (VMamba and Vim) with CNN and Vision Transformer (ViT) architectures, demonstrating that under limited data conditions, Mamba architectures more effectively capture long-range dependencies, achieving a 1.98% increase in mean AUC and a 5.0% increase in accuracy (Nasiri-Sarvi *et al.* 2024). Gagliardi *et al.*, on the other hand, developed a system that concurrently addresses both classification and segmentation tasks, investigating models that simultaneously provide radiologists with a tumor mask and diagnostic information. They identified models that achieved high-performance metrics on the BUSI dataset, including an accuracy exceeding 90%, 92% precision, 90% recall, and a 90% F1 score (Gagliardi *et al.* 2024).

In studies conducted in the realm of breast cancer diagnosis, it is found that hybrid methods and sophisticated CNN architectures have shown promising outcomes. Abhisheka *et al.* pointed out that in isolation DL and ML techniques are commonly inadequate,

and they proposed the Hybrid Breast Cancer Prediction System (HBCPS). This model fuses deep features obtained with ResNet50 with handcrafted features, such as Histogram of Oriented Gradients (HOG), and performs classification using a Support Vector Machine (SVM). The HBCPS model proved to be effective on the BUSI data set, achieving 89.02% accuracy and a 0.8717 AUC score (Abhisheka *et al.* 2025). Similarly, Latha *et al.* used the EfficientNet-B7 architecture and innovative data augmentation techniques to address some accuracy concerns discovered with minority classes and applied appropriate XAI techniques (like Grad-CAM) to promote explainability of the model. Using their methods, the authors achieved classification accuracy of 99.14%, far surpassing the results of previous approaches (Latha *et al.* 2024). Thus, the findings of these studies suggest hybrid modelling and deep CNN architectures with the support of explainable AI, can be successful in classifying breast cancer.

On the other hand, efforts in the literature to enhance segmentation accuracy and improve computational efficiency are also prominent. Umer *et al.* proposed a U-shaped autoencoder-based CNN model equipped with a triple decoder featuring multi-attention mechanisms. They showed that this model, with its ability to capture multi-scale spatial features, achieved Dice scores of 90.45% and 89.13% on the UDIAT and BUSI datasets, respectively (Umer *et al.* 2024). Cai *et al.* developed the SC-Unext model, based on Unext and inspired by cellular apoptosis and division processes, with the aim of reducing computational complexity and model parameter load. This model achieved a Dice score of 75.29% and an accuracy of 97.09% on the BUSI dataset, and was also noted for its fast inference time in CPU environments (Cai *et al.* 2024). Such efficient and lightweight models are considered significant steps toward increasing usability in clinical applications. Thus, this diversity in the literature indicates that AI-based approaches point to a promising future for breast cancer diagnosis, both in terms of accuracy and operational efficiency.

MATERIALS AND METHODS

Dataset

In this study, the publicly available "Breast Cancer Detection" dataset, published by Hayder17 on the Kaggle platform, was utilized for the purpose of detecting breast cancer from mammography images (Kaggle 2025). The dataset consists of pathologically confirmed mammography images divided into two primary classes: benign lesions (labeled as class 0) and malignant lesions (labeled as class 1). Containing a total of 3383 images, with 2225 being benign and 1158 malignant, this rich dataset provides a robust foundation for evaluating the ability of the developed DL models to learn the subtle structural and textural differences between these two critical classes.

To ensure that the model development and evaluation processes are standardized and reproducible, the dataset, comprising 3383 images, was carefully partitioned into training, validation, and testing subsets. This split was performed by allocating 70% of the total dataset (2367 samples) for training, 15% (506 samples) for validation, and the remaining 15% (510 samples) for testing to independently evaluate the final performance of the model. These proportions are intended to ensure the model is trained with sufficient data while also allowing its generalization capability to be reliably measured without overfitting. Furthermore, care was taken to ensure that the class distribution in each subset reflected the proportions of the original dataset. Accordingly, the training set was composed of 1557 benign (0) and 810 malignant (1) samples; the validation set contained 333 benign (0) and 173 malignant

(1) samples; and the test set included 335 benign (0) and 175 malignant (1) samples. The partitioning of the dataset and the class distributions are also detailed in Figure 1.

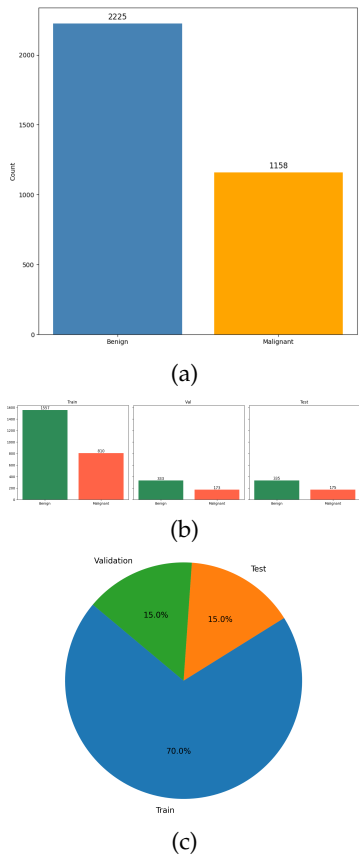


Figure 1 Statistical distribution and partitioning of the "Breast Cancer Detection" dataset. (a) Number of samples for the Benign and Malignant classes in the complete dataset. (b) Class distribution within the training (70%), validation (15%), and testing (15%) subsets. (c) The proportional split of the dataset into training, validation, and test sets.

To better visualize the structure of the dataset and the types of images it contains, representative mammography images for each class (benign and malignant) are presented in Figure 2. As illustrated in Figure 2, benign lesions tend to exhibit smooth and well-defined margins, whereas malignant lesions are more likely to display features such as irregular, indistinct, or spiculated (star-like) borders, higher density, and suspicious microcalcification clusters. In addition to these apparent morphological differences between the classes, these examples also highlight the challenges inherent in mammography, such as low contrast, the potential for dense breast tissue to obscure underlying lesions, and the ambiguities created by overlapping tissue layers. These visual representations aid in understanding the fundamental morphological features that our models must learn and differentiate, and they offer insight into the diversity of the dataset.

Data Augmentation

This study employed a dynamic data augmentation pipeline during training to enhance model generalization and mitigate the risk of overfitting, a common challenge associated with limited medical image datasets. The core strategies of this pipeline, applied

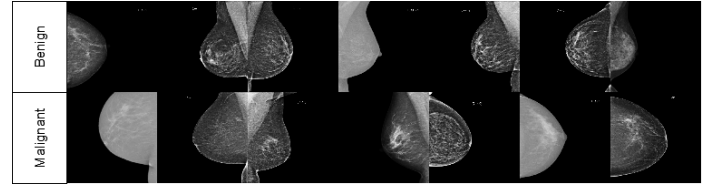


Figure 2 Representative mammogram images illustrating the Benign and Malignant classes.

randomly to each image on-the-fly, are as follows: First, through a "Random Resized Crop" operation, each image was cropped to a random scale of 8% to 100% of its original area with a variable aspect ratio (0.75 to 1.33), and subsequently resized to 224x224 pixels using a random interpolation method. This was complemented by a random horizontal flip, applied with a 50% probability. To introduce chromatic variance, "Color Jitter" was utilized to randomly alter the brightness, contrast, saturation, and hue of the images by a factor of 0.4. Notably, vertical flipping was deliberately excluded from the augmentation strategy.

The purpose of this on-the-fly methodology was to present the model with a diverse and continuously varying stream of data. This approach is designed to discourage the model from memorizing specific artifacts of the training set, thereby fostering a more robust and reliable performance on previously unseen data [Wang et al. \(2024\)](#); [Mumuni et al. \(2024\)](#).

Model Architectures

In order to tackle the problem of automatically classifying breast cancer using mammographic images, this research utilized several important deep CNN architectures. Since there is a common limitation of having little labelled data for the medical domain, we opted to utilize a transfer learning approach. In particular, we are able to utilize the excellent feature representations provided by the pre-trained models from the very large ImageNet database and transfer that knowledge learned onto the small mammogram classification task. The primary motive for this was to speed up the convergence of the model, improve generalization and reduce overfitting. Therefore, in this transfer learning approach, we loaded the initial weights of each architecture to the pre-trained ImageNet version, and we then fine-tuned each model on the breast mammography image dataset.

The first two models we wish to assess are called ResNet50 and DenseNet169, which are both architectures based on different philosophies. ResNet50 is a 50-layer network developed by He et al, and is based on the concept of residual learning. Residual learning allows ResNet50 to prevent the vanishing gradient problem with a very deep neural network. In ResNet50, the vanishing gradient problem is overcome by the addition of shortcut connections into its layers, or what they call "residual blocks" and is considered a solid baseline for classification tasks ([He et al. 2015](#)). DenseNet169, a 169-layer architecture proposed by Huang et al is based on dense connectivity. In this design, each layer receives inputs from all previous layers, making it easier to propagate features and reuse features. It is a unique architecture because of the improvement in parameter efficiency and assumption of improved gradient flow during training ([Huang et al. 2017](#)).

The study included two architectures from the Inception family of Google for their capacity to capture visual information at multiple scales. InceptionV3 uses "Inception modules" which process the input from parallel paths of different sizes of convolutional filters (e.g. 1x1, 3x3, 5x5) and pooling layers. This means that the

output of these paths can be concatenated, allowing the network to learn complex invariances at different resolutions, in addition to optimizations that included the use of factorized convolutions just to name a few. InceptionV4 builds off from InceptionV3 and establishes a more consistent and simple modular structure. It can be thought of as a refinement of the Inception concept, and within InceptionV4, there are a deeper number of blocks that have been more optimized with the intent to achieve greater performance and greater computational efficiency (Szegedy *et al.* 2016).

The strategic selection of these four distinct CNNs ResNet50, DenseNet169, InceptionV3, and InceptionV4 was intended to provide a comprehensive comparison for the task of differentiating between benign, malignant, and normal tissue in mammograms. The rationale is that the unique architectural designs and feature-learning strategies of each model are expected to yield valuable insights into which approach is most effective for this complex medical imaging problem. Through a rigorous analysis of their performance across various evaluation metrics, this study aims to contribute to the growing body of literature on developing automated, deep learning-based systems for the early diagnosis of breast cancer.

Evaluation Metrics

The evaluation of DL models is a fundamental step, indispensable for quantifying their efficacy, justifying methodological choices, and enabling informed, data-centric decision-making. Performance criteria serve multiple critical functions, including gauging the effectiveness of classification models, guiding their optimization, identifying potential errors or biases within the dataset, facilitating comparative analysis between different architectures, and diagnosing issues like overfitting. In the context of this study on breast cancer classification, we have adopted a set of standard evaluation metrics that are well-established and widely accepted within the scientific literature.

The key metrics used in this project i.e. Accuracy, Precision, Recall, and the F1-score have significant importance in scientific fields apart from deep learning. Accuracy is a general measure of performance based on the number of correctly classified instances compared to the total instances given. Precision is simply defined as true positives divided by the number of true positives and false positives and measures the reliability of the model's positive predictions. The higher the precision score, the less the false positives. Recall, or sensitivity, measures whether the model identified all actual positive cases, acting as a measure of completeness. The F1 score is simply the harmonic mean of precision and recall, providing one single metric that weights the trade-off between false positives and false negatives. These definitions are also supported by their mathematical definitions:

$$\text{Accuracy} = \frac{\text{Number of correct predictions}}{\text{Number of total predictions}} \quad (1)$$

$$\text{Precision} = \frac{\text{True Positive}}{\text{True Positive} + \text{False Positive}} \quad (2)$$

$$\text{Recall} = \frac{\text{True Positive}}{\text{True Positive} + \text{False Negative}} \quad (3)$$

$$F_1 = 2 \times \frac{\text{Precision} \times \text{Recall}}{\text{Precision} + \text{Recall}} \quad (4)$$

RESULTS AND DISCUSSION

In this study, the performance and computational complexity of four different CNN architectures were comparatively evaluated for the classification of breast cancer from mammography images. The obtained results are summarized in Table 1. Upon examination of the evaluation metrics, it is clearly evident that the DenseNet169 architecture exhibited superior performance compared to all other models. DenseNet169 achieved the highest score with an accuracy of 73.33%. This model also attained the most successful results with 70.45% precision, 67.83% recall, and a 68.60% F1-score. Subsequently, although the InceptionV3 and ResNet50 models presented identical accuracy rates of 72.16%, they exhibited different profiles in their precision and recall metrics. ResNet50 offered higher precision (69.39% versus 68.96%), while InceptionV3 showed higher recall (66.52% versus 65.02%). This suggests that the two models have different error profiles. Among the tested models, the InceptionV4 architecture exhibited the lowest performance with an accuracy of 70.20%. These findings, based solely on classification performance, establish DenseNet169 as the most suitable architecture for this task.

Table 1 Performance and Complexity of CNN Models for Breast Mammography Image Classification

Model	Acc.	Prec.	Rec.	F1	Params (M)	GFLOPs
DenseNet 169	73.33	70.45	67.83	68.60	12.49	6.72
Inception V3	72.16	68.96	66.52	67.22	21.79	5.67
ResNet 50	72.16	69.39	65.02	65.79	23.51	8.26
Inception V4	70.20	66.60	65.58	65.96	41.15	12.25

Beyond performance metrics, the complexity and computational efficiency of the models play a critical role in evaluating their potential for clinical application. In this context, the most striking finding is that DenseNet169, which demonstrated the highest performance, also possesses the lowest number of parameters among the tested models, with 12.49 million. This indicates that the principles of feature reuse and dense connectivity, which form the foundation of the DenseNet architecture, enable the learning of richer and more discriminative features with fewer parameters. In stark contrast, InceptionV4, which exhibited the lowest performance, is the most complex and computationally expensive model with 41.15 million parameters and 12.24 GFLOPs. This result strongly suggests that in deep learning, a larger and more complex model does not always translate to better performance; in fact, for this specific dataset, it may lead to overfitting or optimization challenges, thereby degrading performance. ResNet50 (23.51M parameters) and InceptionV3 (21.79M parameters) are positioned at a moderate level in terms of complexity, offering a balance between performance and efficiency.

Discussing the results from a clinical perspective reveals the practical value of the models. In medical diagnosis, particularly for life-threatening conditions like cancer, the balance between recall and precision metrics is of vital importance. High recall reduces the likelihood of the model missing malignant cases (false negatives), while high precision prevents the application of unnecessary anxiety and invasive procedures, such as biopsies, to a patient by incorrectly diagnosing a benign case as malignant (false positives). The fact that DenseNet169 achieved the highest scores in both recall and precision metrics indicates that it establishes this critical balance most effectively. Furthermore, its low parameter

count and reasonable GFLOPs value (6.71) facilitate its deployment on systems requiring fewer hardware resources and offer faster inference times, making its integration into the radiologist's workflow practical. Consequently, DenseNet169 emerges as the most promising candidate for development as a decision support system for breast cancer diagnosis, not only for its superior diagnostic accuracy but also for its efficiency and balanced error profile. To analyze the classification capabilities of the InceptionV3 model, which exhibited the highest performance, in more detail, its confusion matrix is presented in Figure 3.

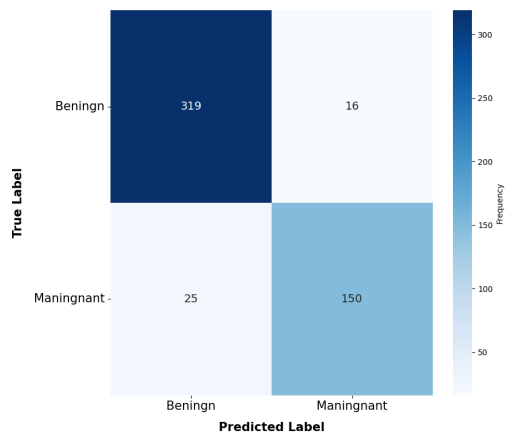


Figure 3 Confusion Matrix of the InceptionV3 Model for Breast Mammography Image Classification.

CONCLUSION

This study aimed to comparatively evaluate the performance and efficiency of four widely-used CNN architectures InceptionV3, DenseNet169, InceptionV4, and ResNet50 for the classification of breast cancer from mammography images. The results obtained unequivocally established that the DenseNet169 model was markedly superior to all other architectures in terms of both diagnostic accuracy and computational efficiency. DenseNet169 exhibited the highest performance with an accuracy of 73.33%, while also proving to be the most lightweight model with 12.49 million parameters. This finding, particularly when contrasted with the lowest performance exhibited by the most complex model, InceptionV4, reinforces the hypothesis that increased model complexity does not invariably lead to better outcomes for this specific task.

Consequently, it is concluded that the principles of dense connectivity and feature reuse inherent in the DenseNet architecture provide a significant advantage in breast cancer classification by enabling the learning of more effective features with fewer resources. While the findings of this study are promising, the limitations of the utilized dataset must be acknowledged. Future work should validate the performance of the DenseNet169 model on larger and more diverse clinical datasets, investigate the impact of different preprocessing and data augmentation techniques, and integrate Explainable Artificial Intelligence (XAI) methods to enhance model interpretability. This research constitutes an important step toward the development of both high-accuracy and efficient AI models and highlights the potential for such systems to be integrated into clinical practice as a reliable decision support tool for radiologists in the future.

Ethical standard

The authors have no relevant financial or non-financial interests to disclose.

Availability of data and material

The data that support the findings of this study are available from the corresponding author upon reasonable request.

Conflicts of interest

The authors declare that there is no conflict of interest regarding the publication of this paper.

LITERATURE CITED

Abhisheka, B., S. K. Biswas, B. Purkayastha, and S. Das, 2025 Integrating deep and handcrafted features for enhanced decision-making assistance in breast cancer diagnosis on ultrasound images. *Multimedia Tools and Applications* pp. 1–23.

Aggarwal, A. and N. Bagri, 2025 Incidence and epidemiology of breast cancer. In *Imaging in Management of Breast Diseases: Volume 1, Overview of Modalities*, pp. 1–9, Springer.

Al-Balas, M., H. Al-Balas, Z. AlAmer, G. Al-Taweel, A. Ghabboun, et al., 2024 Clinical outcomes of screening and diagnostic mammography in a limited resource healthcare system. *BMC Women's Health* **24**: 191.

Alshawwa, I. A., H. Q. El-Mashharawi, F. M. Salman, M. N. A. Al-Qumboz, B. S. Abunasser, et al., 2024 Advancements in early detection of breast cancer: Innovations and future directions .

Bahrami, M., S. H. Hasani, F. Karami, and M. Karami, 2025 Diagnostic values of ultrasound and mammography on prediction of lymphovascular invasion in breast cancer. *Indian Journal of Gynecologic Oncology* **23**: 35.

Bayram, B., I. Kunduracioglu, S. Ince, and I. Pacal, 2025 A systematic review of deep learning in mri-based cerebral vascular occlusion-based brain diseases. *Neuroscience* .

Begum, M. M. M., R. Gupta, B. Sunny, and Z. L. Lutfor, 2024 Advancements in early detection and targeted therapies for breast cancer; a comprehensive analysis. *Asia Pacific Journal of Cancer Research* **1**: 4–13.

Cai, F., J. Wen, F. He, Y. Xia, W. Xu, et al., 2024 Sc-unext: A lightweight image segmentation model with cellular mechanism for breast ultrasound tumor diagnosis. *Journal of Imaging Informatics in Medicine* **37**: 1505–1515.

Cakmak, Y. and I. Pacal, 2025 Enhancing breast cancer diagnosis: A comparative evaluation of machine learning algorithms using the wisconsin dataset. *Journal of Operations Intelligence* **3**: 175–196.

Cakmak, Y., S. Safak, M. A. Bayram, and I. Pacal, 2024 Comprehensive evaluation of machine learning and ann models for breast cancer detection. *Computer and Decision Making: An International Journal* **1**: 84–102.

Chambi, E. A., D. G. Alzamora, and A. A. Salas, 2025 Ultrasonic image processing for the classification of benign and malignant breast tumors: Comparative study of convolutional neural network architectures. *Engineering Proceedings* **83**: 15.

Chandra, M., B. Varghese, and A. Sah, 2025 Mammography and advances. In *Imaging in Management of Breast Diseases: Volume 1, Overview of Modalities*, pp. 35–78, Springer.

Dhamija, E., S. Chandola, and S. Hari, 2025 Contrast-enhanced mammography. In *Imaging in Management of Breast Diseases: Volume 1, Overview of Modalities*, pp. 93–110, Springer.

Gagliardi, M., T. Ruga, E. Vocaturo, and E. Zumpano, 2024 Predictive analysis for early detection of breast cancer through artificial intelligence algorithms. In *International Conference on Innovations in Computational Intelligence and Computer Vision*, pp. 53–70, Springer.

García Megías, I., L. S. Almeida, A. K. Calapaquí Terán, K. M. Pabst, K. Herrmann, *et al.*, 2025 Fapi radiopharmaceuticals in nuclear oncology and theranostics of solid tumours: are we nearer to surrounding the hallmarks of cancer? *Annals of nuclear medicine* pp. 1–17.

He, K., X. Zhang, S. Ren, and J. Sun, 2015 Deep residual learning for image recognition, nd <http://image-net.org/challenges.LSVRC/2015/> (accessed May 24, 2021).

Huang, G., Z. Liu, L. Van Der Maaten, and K. Q. Weinberger, 2017 Densely connected convolutional networks. In *Proceedings of the IEEE conference on computer vision and pattern recognition*, pp. 4700–4708.

İnce, S., I. Kunduracioglu, B. Bayram, and I. Pacal, 2025 U-net-based models for precise brain stroke segmentation. *Chaos Theory and Applications* 7: 50–60.

Islam, M. R., M. M. Rahman, M. S. Ali, A. A. N. Nafi, M. S. Alam, *et al.*, 2024 Enhancing breast cancer segmentation and classification: An ensemble deep convolutional neural network and u-net approach on ultrasound images. *Machine Learning with Applications* 16: 100555.

Kaggle, 2025 Breast cancer.

Katsika, L., E. Boureka, I. Kalogiannidis, I. Tsakiridis, I. Tirodimos, *et al.*, 2024 Screening for breast cancer: a comparative review of guidelines. *Life* 14: 777.

Kiani, P., H. Vatankhahan, A. Zare-Hoseinabadi, F. Ferdosi, S. Ehtiati, *et al.*, 2025 Electrochemical biosensors for early detection of breast cancer. *Clinica Chimica Acta* 564: 119923.

Kim, J., A. Harper, V. McCormack, H. Sung, N. Houssami, *et al.*, 2025 Global patterns and trends in breast cancer incidence and mortality across 185 countries. *Nature Medicine* pp. 1–9.

Koçak, B., A. Ponsiglione, A. Stanzione, C. Bluethgen, J. Santinha, *et al.*, 2025 Bias in artificial intelligence for medical imaging: fundamentals, detection, avoidance, mitigation, challenges, ethics, and prospects. *Diagnostic and Interventional Radiology* 31: 75.

Kurtulus, I. L., M. Lubbad, O. M. D. Yilmaz, K. Kilic, D. Karaboga, *et al.*, 2024 A robust deep learning model for the classification of dental implant brands. *Journal of Stomatology, Oral and Maxillofacial Surgery* 125: 101818.

Latha, M., P. S. Kumar, R. R. Chandrika, T. Mahesh, V. V. Kumar, *et al.*, 2024 Revolutionizing breast ultrasound diagnostics with efficientnet-b7 and explainable ai. *BMC Medical Imaging* 24: 230.

Li, X., L. Zhang, J. Yang, and F. Teng, 2024 Role of artificial intelligence in medical image analysis: A review of current trends and future directions. *Journal of Medical and Biological Engineering* 44: 231–243.

Li, Y., P. Liu, B. Zhang, J. Chen, and Y. Yan, 2025 Global trends and research hotspots in nanodrug delivery systems for breast cancer therapy: a bibliometric analysis (2013–2023). *Discover Oncology* 16: 269.

Lin, H.-Y. and J. Y. Park, 2024 Epidemiology of cancer. In *Anesthesia for oncological surgery*, pp. 11–16, Springer.

Lubbad, M., D. Karaboga, A. Basturk, B. Akay, U. Nalbantoglu, *et al.*, 2024a Machine learning applications in detection and diagnosis of urology cancers: a systematic literature review. *Neural Computing and Applications* 36: 6355–6379.

Lubbad, M. A., I. L. Kurtulus, D. Karaboga, K. Kilic, A. Basturk, *et al.*, 2024b A comparative analysis of deep learning-based approaches for classifying dental implants decision support system. *Journal of Imaging Informatics in Medicine* 37: 2559–2580.

Meng, X., J. Ma, F. Liu, Z. Chen, and T. Zhang, 2024 An interpretable breast ultrasound image classification algorithm based on convolutional neural network and transformer. *Mathematics* 12: 2354.

Mohanti, B. K., P. Mathur, U. Jayarajah, B. M. Biswal, and S. Prinjha, 2025 Introduction to cancer world. In *Radiation Oncology—Principles, Precepts and Practice: Volume I—Technical Aspects*, pp. 1–30, Springer.

Mousa, W. A. E.-F., D. A. A. E.-R. Tolba, and M. M. Moawad, 2024 Diagnostic value of digital breast tomosynthesis in suspicious lesions detected in screening mammogram. *Egyptian Journal of Radiology and Nuclear Medicine* 55: 232.

Mumuni, A., F. Mumuni, and N. K. Gerrar, 2024 A survey of synthetic data augmentation methods in machine vision. *Machine Intelligence Research* 21: 831–869.

Mundel, R., S. Dhadwal, S. Bharti, and M. Chatterjee, 2023 A comprehensive overview of various cancer types and their progression. *Handbook of oncobiology: from basic to clinical sciences* pp. 1–17.

Nasiri-Sarvi, A., M. S. Hosseini, and H. Rivaz, 2024 Vision mamba for classification of breast ultrasound images. In *Deep Breast Workshop on AI and Imaging for Diagnostic and Treatment Challenges in Breast Care*, pp. 148–158, Springer.

Nicosia, L., A. Rotili, F. Pesapane, A. C. Bozzini, O. Battaglia, *et al.*, 2024 Contrast-enhanced mammography (cem) compared to breast magnetic resonance (mri) in the evaluation of breast lobular neoplasia. *Breast Cancer Research and Treatment* 203: 135–143.

Obeagu, E. I. and G. U. Obeagu, 2024 Breast cancer: A review of risk factors and diagnosis. *Medicine* 103: e36905.

Obuchowicz, R., M. Strzelecki, and A. Piórkowski, 2024 Clinical applications of artificial intelligence in medical imaging and image processing—a review.

Ozdemir, B., E. Aslan, and I. Pacal, 2025 Attention enhanced inceptionnext based hybrid deep learning model for lung cancer detection. *IEEE Access*.

Pacal, I., 2025 Diagnostic analysis of various cancer types with artificial intelligence.

Pacal, I., O. Akhan, R. T. Deveci, and M. Deveci, 2025 Nextbrain: Combining local and global feature learning for brain tumor classification. *Brain Research* p. 149762.

Pacal, I. and O. Attallah, 2025 Inceptionnext-transformer: A novel multi-scale deep feature learning architecture for multimodal breast cancer diagnosis. *Biomedical Signal Processing and Control* 110: 108116.

Rezaei, F., A. Mazidimoradi, Z. Pasokh, F. Mobasher, A. Taheri, *et al.*, 2025 Global trend of breast cancer among women aged 55 and older from 2010 to 2019: An analysis by socio-demographic index and geographic regions. *Indian Journal of Gynecologic Oncology* 23: 1–18.

Siqueira, P. B., M. M. de Sousa Rodrigues, Í. S. S. de Amorim, T. G. da Silva, M. da Silva Oliveira, *et al.*, 2024 The ape1/ref-1 and the hallmarks of cancer. *Molecular Biology Reports* 51: 47.

Sirvi, P. K., V. Jadhav, G. Paul, R. Jain, and A. K. Yadav, 2025 Therapeutic hallmarks of cancer and immunology. In *Nanotechnology Based Strategies for Cancer Immunotherapy: Concepts, Design, and Clinical Applications*, pp. 21–53, Springer.

Szegedy, C., V. Vanhoucke, S. Ioffe, J. Shlens, and Z. Wojna, 2016 Rethinking the inception architecture for computer vision. In

Proceedings of the IEEE conference on computer vision and pattern recognition, pp. 2818–2826.

Trentham-Dietz, A., C. H. Chapman, J. Jayasekera, K. P. Lowry, B. M. Heckman-Stoddard, *et al.*, 2024 Collaborative modeling to compare different breast cancer screening strategies: a decision analysis for the us preventive services task force. *JAMA* **331**: 1947–1960.

Umer, M. J., M. Sharif, and M. Raza, 2024 A multi-attention triple decoder deep convolution network for breast cancer segmentation using ultrasound images. *Cognitive Computation* **16**: 581–594.

Wang, Z., P. Wang, K. Liu, P. Wang, Y. Fu, *et al.*, 2024 A comprehensive survey on data augmentation. *arXiv preprint arXiv:2405.09591*.

Xiong, X., L.-W. Zheng, Y. Ding, Y.-F. Chen, Y.-W. Cai, *et al.*, 2025 Breast cancer: pathogenesis and treatments. *Signal transduction and targeted therapy* **10**: 49.

Yousefnia, S., 2024 Breast cancer, subtypes, risk factors, and treatment. In *The Palgrave Encyclopedia of Disability*, pp. 1–14, Springer.

Zeynalov, J., Y. Çakmak, and İ. Paçal, 2025 Automated apple leaf disease classification using deep convolutional neural networks: A comparative study on the plant village dataset. *Journal of Computer Science and Digital Technologies* **1**: 5–17.

Zuo, W.-F., Q. Pang, X. Zhu, Q.-Q. Yang, Q. Zhao, *et al.*, 2024 Heat shock proteins as hallmarks of cancer: insights from molecular mechanisms to therapeutic strategies. *Journal of Hematology & Oncology* **17**: 81.

How to cite this article: Cakmak, Y., and Zeynalov, J. A Comparative Analysis of Convolutional Neural Network Architectures for Breast Cancer Classification from Mammograms. *Artificial Intelligence in Applied Sciences*, 1(1), 28-34, 2025.

Licensing Policy: The published articles in AIAPP are licensed under a [Creative Commons Attribution-NonCommercial 4.0 International License](#).

